BIOCHEMISTRY

 Volume 44, Number 45 November 15, 2005

New Concepts

Rhodopsin Activation Follows Precoupling with Transducin: Inferences from Computational Analysis[†,‡]

Francesca Fanelli* and Daniele Dell'Orco

Department of Chemistry, University of Modena and Reggio Emilia, and Dulbecco Telethon Institute, via Campi 183 41100 Modena, Italy

Received August 2, 2005; Revised Manuscript Received September 15, 2005

ABSTRACT: The electrostatic and shape complementarities between the crystal structures of dark rhodopsin and heterotrimeric transducin (Gt) have been evaluated by exhaustively sampling the roto-translational space of one protein with respect to the other. Structural complementarity, reliability, and consistency with in vitro evidence all converge in the same rhodopsin−Gt complex, showing that the functionally important R135 of the E/DRY motif is almost accessible to the C-terminus of Gt_α already in the dark state. The main inference from this study is that activation of rhodopsin and Gt may be concurrent processes, consisting of conformational changes in a supramolecular complex formed prior to the light-induced activation of the photoreceptor.

Dark Rhodopsin Has the Determinants for Recognizing Heterotrimeric Transducin: Evidence from in Vitro Experiments

Of the different states that define the reaction path of rhodopsin activation, the dark or ground state is the only one known at the atomic detail (*1*−*5*). At least four intermediates intervene between dark rhodopsin and Meta II (MII),[1] the signaling state capable of activating heterotrimeric G protein (i.e., transducin (Gt)) (*6*). The 5.5 Å electron density map of Meta I (MI), the photostationary state that precedes MII, has been recently released, providing evidence that rhodopsin remains in a conformation similar to that of the ground state until late in the photobleaching process and that the gross conformational changes occur during the MI to MII transition (*7*).

It is widely thought that rhodopsin binds Gt in the MII state (*6*). The patchwork of the most relevant information from in vitro experiments on rhodopsin−transducin recognition suggests that the $\alpha 4/\beta 6$ loop and the C-terminus of Gt_α recognize a solvent-accessible cleft on MII, formed by amino acids from the cytosolic extensions of H3, H5, and H6 (the letter "H" stands for "helix"), from the N-terminus of the second intracellular loop (I2), and from the N-terminus of H8 (reviewed in refs *8*−*10*). Recent experiments have demonstrated that the role of H6 movements during MII formation is to provide a binding site on the cytoplasmic face of rhodopsin for the Gt_α C-terminus (*11*). This movement appears to open a cleft and expose a hydrophobic patch,

[†] This study was supported by a Telethon-Italy Grant No. S00068TELA (To F.F.).

[‡] The coordinates of the selected complexes involving Gt_mut1, Gt_mut2, Gt_mut3, Gt_chim1, and Gt_chim2 will be released upon request.

* Corresponding author. Phone: +39 059 2055114. Fax: +39 059 373543. E-mail: fanelli@unimo.it.

[1] Abbreviations: Gt, transducin; MII, Meta II; MI, Meta I; I2, second intracellular loop; PWR, plasmon-waveguide resonance; GPCRs, G protein-coupled receptors; PDB, Protein Data Bank; C_α-RMSD, C_α-atom root mean square deviation; I3, third intracellular loop.

10.1021/bi051537y CCC: $30.25
Published on Web 10/22/2005

which directly interacts with the Gt_α C-terminus and increases the affinity for transducin. In line with the evidence that MII is the rhodopsin state intended for recognizing Gt, the few computational models of rhodopsin−Gt interaction, reported so far, employed an active-state model of rhodopsin (*12*−*16*).

Despite the commonly accepted knowledge that recruitment of Gt would follow rhodopsin activation, experimental evidence that dark rhodopsin and heterotrimeric transducin may exist as a preformed complex have appeared early in the literature, though not pursued any further (*17*). Also in line with this evidence is the observation that dark rhodopsin has a low basal activity (reviewed in ref *6*) and that proton uptake from the cytosol, associated with MII formation, requires the presence of transducin to occur (*18*). Other evidence comes from surface modification and mass spectrometry (*19*) as well as from plasmon-waveguide resonance spectroscopy (PWR) determinations (*20*, *21*). PWR spectroscopy experiments, in fact, showed that the affinity of dark rhodopsin for heterotrimeric Gt is 64 nM. Collectively, these data suggest that MII formation may depend on the presence of transducin and that the rhodopsin−transducin complex is already formed in the dark. The hypothesis that not only rhodopsin but also the homologous G protein-coupled receptors (GPCRs) and G proteins are "constitutively coupled" or precoupled is supported by PWR determinations, which provided evidence for a direct interaction (i.e., with a 60 nM K_D) between ligand-free δ-opioid receptor and its cognate G protein (*22*).

The structural model of dark rhodopsin is not in contrast with this hypothesis, as the putative recognition points for transducin (i.e., I2 and the core-facing amino acids in the cytosolic extensions of H3, H5, and H6; reviewed in refs *8*−*10*) are significantly exposed to the solvent (*2*).

Exploring the Structural Complementarity between Dark Rhodopsin and Gt by Rigid-Body Docking

Here, we test the hypothesis that dark rhodopsin has the potential to recognize Gt and that rhodopsin−Gt coupling occurs prior to MII formation.

The analysis of the structural complementarity between the cytosolic domains of dark rhodopsin and heterotrimeric Gt was done by exhaustively sampling the roto-translational space of one protein (probe) with respect to the other (target). Dark rhodopsin structure (PDB code: 1U19 (*2*)) was used as fixed protein (i.e., target), whereas heterotrimeric Gt was allowed to explore all the possible orientations around the cytosolic domains of the target (i.e., probe). The rigid-body docking algorithm ZDOCK was employed, which has already proven effectiveness in structure predictions of protein−protein complexes (*23*). While neglecting the conformational changes that may accompany protein−protein interaction is a drawback in some cases, in this case, the rigid-body approximation is rather a requirement as we want to investigate whether any reliable complementarity exists between the crystal structure of dark rhodopsin and Gt, independently of possible conformational rearrangements. However, introduction of differences in the side chain and/or backbone conformation and/or in the amino acid length of the N- and C-termini of the different G protein subunits was probed as well to infer the degree of tolerance of the rigid-body docking algorithm to such structural changes. Thus, different heterotrimeric structures were probed. The first probed heterotrimer, Gt_chim1, was a modified version of the crystal structure of $Gt_{\alpha\beta1\gamma1}$ (i.e., a $Gt_\alpha/Gi_{\alpha1}$ chimera, in which residues 216−294 of Gt_α were replaced with the corresponding residues (220−298) from $Gi_{\alpha1}$; PDB code: 1GOT (*24*)). Structural modifications consisted of the addition of the NMR structure of the last 12 amino acids of the α-subunit (i.e., PDB code: 1AQG (*25*)) and completion of the C-terminus of the γ-subunit, whose last 12 amino acids were modeled in α-helix. These conformations of the C-termini of both α- and γ-subunits are thought to be held by the receptor-bound form of the peptides (*25*, *26*). Alternative conformations of the C-termini of Gt_α and Gt_γ were probed as well (results not shown). The γ-subunit in Gt_chim1 was extracted from the $Gt_{\beta\gamma}$-fosducin complex (PDB code 1A0R) (*27*). The rationale for using the γ-subunit from the $\beta\gamma$-fosducin complex was essentially to probe the effect of differences in the side chain and, by a lower extent, in the main chain conformation of such subunit on the docking results. Modified versions of Gt_chim1 were also probed that are (a) one holding the original β- and γ-subunits from 1GOT structure, i.e., with incomplete terminations (Gt_chim2); (b) one holding a side chain energy minimized form of the α- and β-subunits from a previous study (*28*) (i.e., Gt_chim3); and (c) mutated forms of Gt_chim1 and Gt_chim2, holding the bovine Gt_α sequence (i.e., Gt_mut1 and Gt_mut2). Finally, a variant form of Gt_mut2 has been also probed, holding a complete Gt_γ C-term with the last 12 amino acids modeled in α-helix (Gt_mut3). Dimeric and tetrameric forms of the 1U19 structure were also used as targets in other simulations. These models were achieved by fitting the 1U19 structure into each monomer in the semiempirical oligomeric model of rhodopsin recently released (i.e., PDB code: 1N3M) (*29*).

To improve sampling efficiency, the rhodopsin portions 1−59, 76−130, 157−220, and 252−308, corresponding to the transmembrane and extracellular domains, were not taken into account in docking simulations. A rotational sampling interval of 6° was employed, and the best 4000 solutions were retained and ranked according to the ZDOCK score, a summation over three scoring functions, i.e., the pairwise shape complementarity, desolvation, and electrostatics. To filter the most reliable solutions among the 4000 best scored ones, i.e., the Gt orientations fulfilling the membrane topology requirements, the low resolution information from in vitro experiments on MII−transducin interactions were translated into broad $C_\alpha-C_\alpha$ intermolecular distance constraints, i.e., (a) lower than 15.0 Å between rhodopsin-S240 and both Gt_α-N343 and Gt_α-D311; (b) lower than 20.0 Å between rhodopsin-R135 and Gt_α-F350; and (c) lower than 20.0 Å between rhodopsin-Q312 and Gt_α-K345. In detail, the distance-based filters reported in (a) take broadly into account the information from cysteine cross-linking experiments between activated rhodopsin and Gt (*30*, *31*); the distance-base filter in (b) properly accounts for the wide experimental evidence that the C-terminus of Gt_α docks between the cytosolic extensions of H3 and H6, close to the E/DRY motif (reviewed in refs *8*−*10*); finally, the distance-based filter in (c) accounts for the hypothesized interactions between the N310-Q312 region (H8) of rhodopsin and the last 10 amino acids of Gt_α (*32*, *33*).

The solutions fulfilling at least one of the three distance constraints were collected and subjected to cluster analysis by using an algorithm from Dr. M. Schaefer (Michael Schaefer, Syngenta Crop Protection AG, unpublished work), followed by visual analysis of the centers (i.e., the solution representative of each clusters) of the most populated clusters. A C_α-atom root mean square deviation (C_α-RMSD) of 3.0 Å was employed for clustering, following an optimization procedure recently reported (*34*). In detail, to aid the selection of the most appropriate C_α-RMSD, the dispersion index σ^2 was used, that is the variance of the statistical distribution of each structure in the cluster. Hence, if cluster i groups N_k structures, each indicated by p, its homogeneity may be described by

$$\sigma_i^2 = \frac{1}{N_k}\sum_{p=1}^{N_k}(\mathrm{RMSD}_p - \overline{\mathrm{RMSD}_i})^2$$

where $\overline{\mathrm{RMSD}_i}$ indicates the average C_α-RMSD among the structures of cluster i. Clusters with reasonably low σ^2 are, with higher confidence than clusters with high index, represented by their center, which by definition has a null RMSD. Because of its definition, σ^2 square-rooted can be directly compared with the threshold chosen for running the cluster analysis. Our data suggest that σ values should not significantly exceed 1.0 Å, as an indicative value.

Energy minimizations of the selected rhodopsin−Gt complexes were done by means of CHARMM (*35*), by employing the IMM1 implicit water/membrane model (*36*). Energy minimizations were carried out by using 1500 steps of steepest descent followed by a conjugate gradient minimization, until the root-mean-square gradient was less than 0.001 kcal/mol Å. The adjustable parameter "a" and the nonpolar core thickness were set equal to 0.85 and 32 Å, respectively. The "united atom approximation" was employed. All the backbone atoms except those of the last 10 amino acids of Gt_α were kept fixed during energy minimization. Furthermore, side chain energy minimizations concerned the amino acids at the receptor−G protein interface including the last 10 amino acids of Gt_α.

Dark Rhodopsin Has the Determinants for Recognizing Heterotrimeric Transducin: Insights from in Silico Experiments

Regardless of the differences in the side chain conformation and in the length of the C-terminus of the γ-subunit (i.e., full length or lacking the first eight and last five amino acids), the best scored docking solution, from each run, fulfilling most of the distance-based filters is also consistent with the expected membrane topology of Gt (see Figure 2 legend for details on the filtered $C_\alpha-C_\alpha$ distances in the selected complex between rhodopsin and Gt_mut1). Acceptable membrane topologies were considered those characterized by the main axis of the N-terminal α-helix of Gt_α (i.e., αN) almost parallel and close enough to the membrane surface to allow the hydrophobic N-acyl and farnesyl modifications of the α- and γ-subunit, respectively, to insert into the membrane. For each of the different docking runs, the number of filtered solutions fell between 500 and 700 out of 4000 and included all the solutions holding an acceptable membrane topology of Gt, i.e., realistic solutions (Table 1). In this respect, one of the features of these distance-based filters is to discard most of the high score solutions, which violated the membrane topology of Gt (i.e., false positives). Cluster analysis on the filtered solutions followed by visual inspection of the cluster centers completed the rejection of false positives. On average, the realistic solutions constitute less than 2% of the total 4000 solutions and 9% of the filtered solutions (Table 1).

Table 1: Docking Results Probing Different Structural Models of Heterotrimeric Transducin

predicted complex[a]	filtered solutions[b]	%[c]	best solution[d]	ZDOCK_{best}[e]	C_α-RMSD[f] (Å)
Rho-Gt_mut1	581	12	12	60.86	
Rho-Gt_mut2	644	11	14	60.15	0.30
Rho-Gt_mut3	604	12	10	60.18	0.74
Rho-Gt_chim1	628	10	20	58.61	0.03
Rho-Gt_chim2	670	7	23	57.52	0.72
Rho-Gt_chim3	510	7	21	56.47	0.04

[a] Predicted rhodopsin−Gt complex using different Gt models (see text for details). [b] Number of solutions resulting from the distance-based filtering. [c] Percentage of realistic solutions among those resulting from the distance-based filtering. [d] Position of the highest scored solution in the output list (i.e., made of 4000 solutions). [e] ZDOCK score of the selected solution. [f] C_α-RMSD (Å) between each energy-minimized selected complex and Gt_mut1, i.e., the complex shown in Figures 1 and 2. All the C_α-atoms have been considered in RMSDs calculations, except for rhodopsin-Gt_mut2, rhodopsin-Gt_mut3, and rhodopsin-Gt_chim2 complexes, for which the γ-subunit was excluded from calculations, due to the slight differences in main chain conformation concerning such subunits in Gt_mut1, on one hand, and Gt_mut2, Gt_mut3, and Gt_chim2, on the other one.

Despite the structural differences in the heterotrimers used as probes in the different docking simulations, the C_α-RMSD of the best scored realistic solutions from each run was close to zero (Table 1). This proves some tolerance of the ZDOCK algorithm to changes in side chain and/or backbone conformation of the different G protein subunits, providing more strength to predictions. In the predicted complex, the C-terminus of Gt_α makes contacts with I2, the cytosolic extensions of H3 and H6, as well as with H8 and the C-terminus of rhodopsin (Figures 1 and 2). Furthermore, (a) the α3/β5 loop of Gt_α interacts with the C-terminus of rhodopsin (Figure 1); (b) the α4/β6 loop of Gt_α makes contacts with both the third intracellular loop (I3) and the C-terminus of rhodopsin; and (c) the C-terminus of rhodopsin is also involved in contacts with the N-terminus of Gt_α and with limited portions of Gt_β (Figure 1). The functionally important R135 of the E/DRY motif is almost accessible to the C-terminus of Gt_α already in the dark state. In fact, the $C_\alpha-C_\alpha$ distance between the E/DRY arginine and F350 of Gt_α is 7.9 Å. Therefore, a limited energy minimization of the rhodopsin−Gt complex reveals the possibility for R135 to switch from the intramolecular salt bridge with E247 to an intermolecular interaction with the backbone carboxylate of Gt_α, i.e., that of F350 (Figure 2a,b). This is concurrent with the establishment of a salt bridge between E247 of rhodopsin and K345 of Gt_α (Figure 2a,b). This interaction pattern results in the most reliable one regardless of the side chain conformations of $Gt_{\alpha\beta}$, as well as of the length and side chain and main chain conformations of Gt_γ. It is worth noting that wild-type Gt_α and the $Gt_\alpha/Gi_{\alpha1}$ chimera produce identical best complexes (Table 1), consistent with their similar functional behavior (*24*).

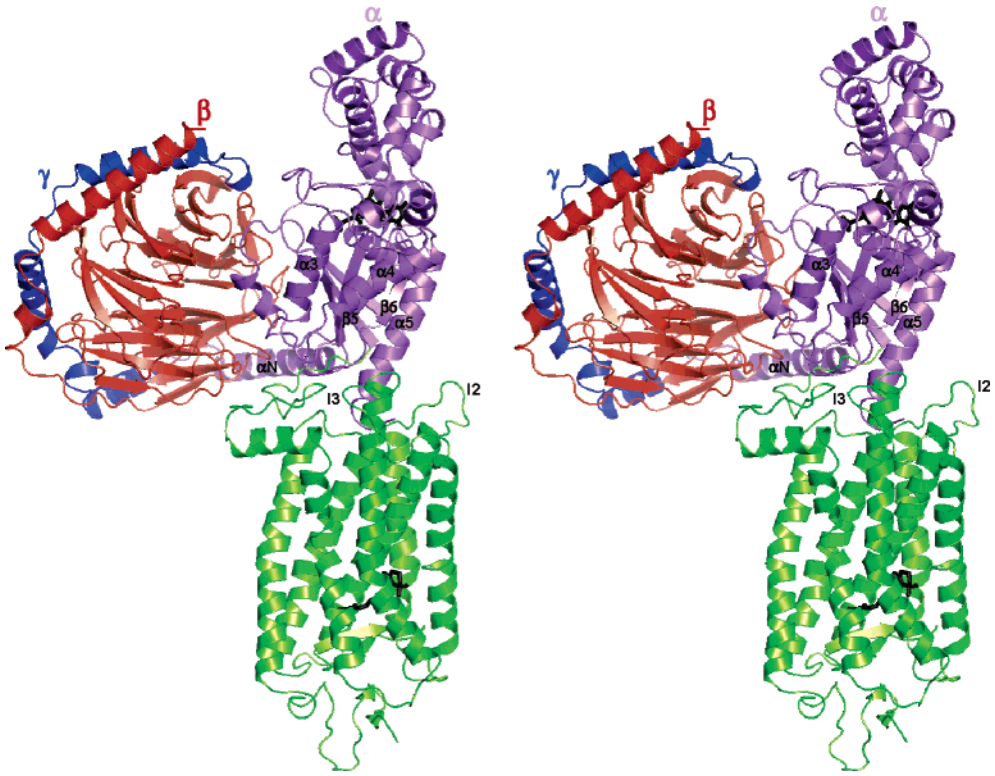

FIGURE 1: Stereoview, in a direction parallel to the membrane surface, of the energy minimized complex between monomeric dark rhodopsin and Gt_mut1. Rhodopsin is in yellow green, whereas the α-, *β*-, and *γ*-subunits of Gt are in violet, orange, and blue, respectively. Black sticks indicate retinal and GDP.

The gross orientation of Gt with respect to rhodopsin in our selected complexes is similar to that of a computational model previously proposed (*13*). Similarities, which also concern the location of the N- and C-termini of Gt_α, occur despite the differences in the structural models employed in the two studies. In contrast, the membrane topology of transducin in the rhodopsin−Gt complex predicted by our computational experiments differs from that proposed by Chabre and le Marie (*16*). In fact, in our complex, the main axis of the αN is almost parallel to the putative membrane, whereas in that by Chabre and le Marie αN hangs off at a large angle from the membrane plane (*16*). The membrane topology of transducin as inferred from ours and other studies (*8*, *9*, *13*) is supported by previous electrostatic potential calculations showing that the solvent-exposed surface of αN has a positive electrostatic potential that can complement the negative potential of phospholipids. Such a positive isopotential surface is enlarged by the presence of the *β*-subunit that contributes to neutralize negative charges on αN (*28*).

Despite the proved tolerance to side chain and backbone conformational changes, the rigid-body docking approach does not allow changes in the internal degrees of freedom of the interacting proteins. Thus, the fact that the complexes, from each run, which fulfill at best experimentally based distance constraints and membrane topology requirements fall among the top 23 out of the best 4000 solutions (Table 1), is strongly supportive of the hypothesis that dark rhodopsin has the potential to recognize GDP-bound heterotrimeric Gt. The excellent convergence between the results of different docking runs employing a number of structural variances of Gt provides more strength to such predictions.

Our results are also consistent with the evidence from PWR spectroscopy experiments showing that dark rhodopsin has a free energy of association (ΔG^0_{as}) with Gt only 2.6 kcal/mol less negative than that of MII (i.e., -9.9 ± 0.1 kcal/mol versus -12.5 ± 0.1 kcal/mol, respectively) (*21*). Interestingly, the architecture of the selected complex between monomeric rhodopsin and heterotrimeric Gt (i.e., 1:1 stoichiometry, Figure 1) is also one of the few best scored and reliable solutions resulting from the docking of Gt with either the dimeric or tetrameric forms of the photoreceptor (results not shown). The rhodopsin dimer and tetramer employed in this study hold the same architecture as that in a semiempirical oligomeric model recently proposed (PDB code 1N3M) (*29*). Other reliable solutions include those characterized by contacts between two rhodopsin molecules and one heterotrimeric Gt (i.e., 2:1 stoichiometry). A worthy result is that, regardless of whether rhodopsin is monomeric or oligomeric, in all the most reliable rhodopsin−transducin complexes, the C-terminus of Gt_α docks into the same site of the photoreceptor, approaching the highly conserved and functionally important E/DRY motif (Figure 2a,b). Collectively, these results suggest that the receptor monomer holds the structural determinants for G protein activation, consistent with the results of functional characterization of rhodopsin monomers and dimers in detergents demonstrating that monomeric rhodopsin can activate transducin, although the oligomeric form is more active (*37*).

In conclusion, the results of our study suggest that dark rhodopsin has the potential to recognize heterotrimeric transducin. The main implication is that rhodopsin activation occurs following precoupling to Gt. This means that all the rhodopsin intermediates from the dark to the MI states, which

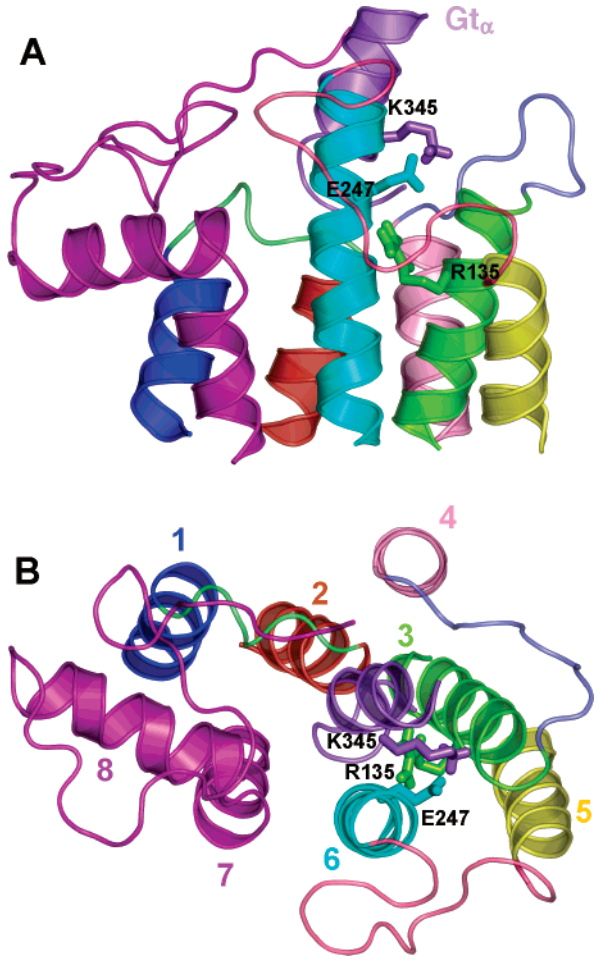

FIGURE 2: Two views of the energy minimized complex between monomeric dark rhodopsin and Gt_mut1, in a direction (a) parallel and (b) perpendicular to the membrane surface of the cytosolic half of rhodopsin and of the last 14 amino acids of Gt_α. Different colors indicate the seven helices, the three intracellular loops, and the C-terminus of rhodopsin. Sticks represent the side chains of R135 and E247 from rhodopsin and of K345 from Gt_α. In this complex, the $C_\alpha-C_\alpha$ intermolecular distances employed by the different filters are i.e., (a) 16.2 and 13.9 Å between rhodopsin-S240 and Gt_α-N343 and Gt_α-D311, respectively; (b) 7.9 Å between rhodopsin-R135 and Gt_α-F350; and (c) 12.3 Å between rhodopsin-Q312 and Gt_α-K345. Drawings were done by means of the software PYMOL 0.97 (http://pymol.sourceforge.net/).

are expected to share the same arrangements of the cytosolic domains (*7*), are always in complex with Gt. Therefore, the structural changes, which accompany MI to MII transition and take about 1 ms to occur, may be catalyzed by Gt. In this framework, the small difference in the association free energy concerning dark rhodopsin−Gt and MII−Gt complexes may be essentially the isomerization energy necessary for the receptor to improve contacts with the G-protein portions intended for transferring signals to the GDP binding site. Interestingly, the G-protein portions suggested by in vitro evidence to mediate the structural information transfer from the receptor to the GDP binding site (reviewed in refs *8*−*10*) include the $\alpha4/\beta6$ loop and the C-terminus of Gt_α, which make most of the rhodopsin−Gt interface in our model. Activation of rhodopsin and Gt may be concurrent processes, consisting of conformational changes in a supramolecular complex formed prior to light-induced activation of the photoreceptor. In this respect, the rhodopsin−Gt interaction model herein presented may be considered as the starting point for computational investigations of such processes.

ACKNOWLEDGMENT

We are extremely grateful to Pier G. De Benedetti and Tommaso Costa for critical discussion.

REFERENCES

1. Palczewski, K., Kumasaka, T., Hori, T., Behnke, C. A., Motoshima, H., Fox, B. A., Le Trong, I., Teller, D. C., Okada, T., Stenkamp, R. E., Yamamoto, M., and Miyano, M. (2000) Crystal structure of rhodopsin: A G protein-coupled receptor, *Science 289*, 739−745.
2. Okada, T., Sugihara, M., Bondar, A. N., Elstner, M., Entel, P., and Buss, V. (2004) The retinal conformation and its environment in rhodopsin in light of a new 2.2 Å crystal structure, *J. Mol. Biol. 342*, 571−583.
3. Li, J., Edwards, P. C., Burghammer, M., Villa, C., and Schertler, G. F. (2004) Structure of bovine rhodopsin in a trigonal crystal form, *J. Mol. Biol. 343*, 1409−1438.
4. Okada, T., Fujiyoshi, Y., Silow, M., Navarro, J., Landau, E. M., and Shichida, Y. (2002) Functional role of internal water molecules in rhodopsin revealed by X-ray crystallography, *Proc. Natl. Acad. Sci. U.S.A. 99*, 5982−5987.
5. Teller, D. C., Okada, T., Behnke, C. A., Palczewski, K., and Stenkamp, R. E. (2001) Advances in determination of a high-resolution three-dimensional structure of rhodopsin, a model of G-protein-coupled receptors (GPCRs), *Biochemistry 40*, 7761−7772.
6. Okada, T., Ernst, O. P., Palczewski, K., and Hofmann, K. P. (2001) Activation of rhodopsin: new insights from structural and biochemical studies, *Trends Biochem. Sci. 26*, 318−324.
7. Ruprecht, J. J., Mielke, T., Vogel, R., Villa, C., and Schertler, G. F. (2004) Electron crystallography reveals the structure of metarhodopsin I, *EMBO J. 23*, 3609−3620.
8. Bourne, H. R. (1997) How receptors talk to trimeric G proteins, *Curr. Opin. Cell Biol. 9*, 134−142.
9. Hamm, H. E. (2001) How activated receptors couple to G proteins, *Proc. Natl. Acad. Sci. U.S.A. 98*, 4819−4821.
10. Fanelli, F., and De Benedetti, P. G. (2005) Computational modeling approaches to Structure−Function Analysis of G Protein-Coupled Receptors, *Chem. Rev. 105*, 3297−3351.
11. Janz, J. M., and Farrens, D. L. (2004) Rhodopsin activation exposes a key hydrophobic binding site for the transducin alpha-subunit C terminus, *J. Biol. Chem. 279*, 29767−29773.
12. Filipek, S., Krzysko, K. A., Fotiadis, D., Liang, Y., Saperstein, D. A., Engel, A., and Palczewski, K. (2004) A concept for G protein activation by G protein-coupled receptor dimers: the transducin/rhodopsin interface, *Photochem. Photobiol. Sci. 3*, 628−638.
13. Slusarz, R., and Ciarkowski, J. (2004) Interaction of class A G protein-coupled receptors with G proteins, *Acta Biochim. Pol. 51*, 129−136.
14. Ciarkowski, J., Witt, M., and Slusarz, R. (2005) A hypothesis for GPCR activation, *J. Mol. Model.*, published online May 12, 2005, http://dx.doi.org/10.1007/s00894-005-0270-9.
15. Yeagle, P. L., and Albert, A. D. (2003) A conformational trigger for activation of a G protein by a G protein-coupled receptor, *Biochemistry 42*, 1365−1368.
16. Chabre, M., and le Maire, M. (2005) Monomeric G-Protein-Coupled Receptor as a Functional Unit, *Biochemistry 44*, 9395−9403.
17. Hamm, H. E., Deretic, D., Hofmann, K. P., Schleicher, A., and Kohl, B. (1987) Mechanism of action of monoclonal antibodies that block the light activation of the guanyl nucleotide-binding protein, transducin, *J. Biol. Chem. 262*, 10831−10838.
18. Fahmy, K., Sakmar, T. P., and Siebert, F. (2000) Transducin-dependent protonation of glutamic acid 134 in rhodopsin, *Biochemistry 39*, 10607−10612.
19. Wang, X., Kim, S. H., Ablonczy, Z., Crouch, R. K., and Knapp, D. R. (2004) Probing rhodopsin-transducin interactions by surface modification and mass spectrometry, *Biochemistry 43*, 11153−11162.

20. Salamon, Z., Wang, Y., Soulages, J. L., Brown, M. F., and Tollin, G. (1996) Surface plasmon resonance spectroscopy studies of membrane proteins: transducin binding and activation by rhodopsin monitored in thin membrane films, *Biophys. J. 71*, 283−294.
21. Alves, I. D., Salgado, G. F., Salamon, Z., Brown, M. F., Tollin, G., and Hruby, V. J. (2005) Phosphatidylethanolamine enhances rhodopsin photoactivation and transducin binding in a solid supported lipid bilayer as determined using plasmon-waveguide resonance spectroscopy, *Biophys. J. 88*, 198−210.
22. Alves, I. D., Salamon, Z., Varga, E., Yamamura, H. I., Tollin, G., and Hruby, V. J. (2003) Direct observation of G-protein binding to the human delta-opioid receptor using plasmon-waveguide resonance spectroscopy, *J. Biol. Chem. 278*, 48890−48897.
23. Chen, R., Li, L., and Weng, Z. (2003) ZDOCK: an initial-stage protein-docking algorithm, *Proteins 52*, 80−87.
24. Lambright, D. G., Sondek, J., Bohm, A., Skiba, N. P., Hamm, H. E., and Sigler, P. B. (1996) The 2.0 Å crystal structure of a heterotrimeric G protein, *Nature 379*, 311−319.
25. Kisselev, O. G., Kao, J., Ponder, J. W., Fann, Y. C., Gautam, N., and Marshall, G. R. (1998) Light-activated rhodopsin induces structural binding motif in G protein alpha subunit, *Proc. Natl. Acad. Sci. U.S.A. 95*, 4270−4275.
26. Kisselev, O. G., and Downs, M. A. (2003) Rhodopsin controls a conformational switch on the transducin gamma subunit, *Structure 11*, 367−373.
27. Loew, A., Ho, Y. K., Blundell, T., and Bax, B. (1998) Phosducin induces a structural change in transducin beta gamma, *Structure 6*, 1007−1019.
28. Fanelli, F., Menziani, C., Scheer, A., Cotecchia, S., and De Benedetti, P. G. (1999) Theoretical study of the electrostatically driven step of receptor-G protein recognition, *Proteins 37*, 145−156.
29. Liang, Y., Fotiadis, D., Filipek, S., Saperstein, D. A., Palczewski, K., and Engel, A. (2003) Organization of the G protein-coupled receptors rhodopsin and opsin in native membranes, *J. Biol. Chem. 278*, 21655−21662.
30. Cai, K., Itoh, Y., and Khorana, H. G. (2001) Mapping of contact sites in complex formation between transducin and light-activated rhodopsin by covalent crosslinking: use of a photoactivatable reagent, *Proc. Natl. Acad. Sci. U.S.A. 98*, 4877−4882.
31. Itoh, Y., Cai, K., and Khorana, H. G. (2001) Mapping of contact sites in complex formation between light-activated rhodopsin and transducin by covalent crosslinking: use of a chemically preactivated reagent, *Proc. Natl. Acad. Sci. U. S.A. 98*, 4883−4887.
32. Ernst, O. P., Meyer, C. K., Marin, E. P., Henklein, P., Fu, W. Y., Sakmar, T. P., and Hofmann, K. P. (2000) Mutation of the fourth cytoplasmic loop of rhodopsin affects binding of transducin and peptides derived from the carboxyl-terminal sequences of transducin alpha and gamma subunits, *J. Biol. Chem. 275*, 1937−1943.
33. Marin, E. P., Krishna, A. G., Zvyaga, T. A., Isele, J., Siebert, F., and Sakmar, T. P. (2000) The amino terminus of the fourth cytoplasmic loop of rhodopsin modulates rhodopsin-transducin interaction, *J. Biol. Chem. 275*, 1930−1936.
34. Dell'Orco, D., Seeber, M., De Benedetti, P., and Fanelli, F. (2005) Probing fragment complementation by rigid-body docking: In silico reconstitution of calbindin D9k. *J. Chem. Inf. Model. 45*, 1429−1438.
35. Brooks, B. R., Bruccoleri, R. E., Olafson, B. D., States, D. J., Swaminathan, S., and Karplus, M. (1983) Charmm: a program for macromolecular energy, minimization and dynamics calculations, *J. Comput. Chem. 4*, 187−217.
36. Lazaridis, T. (2003) Effective energy function for proteins in lipid membranes, *Proteins 52*, 176−192.
37. Jastrzebska, B., Maeda, T., Zhu, L., Fotiadis, D., Filipek, S., Engel, A., Stenkamp, R. E., and Palczewski, K. (2004) Functional characterization of rhodopsin monomers and dimers in detergents, *J. Biol. Chem. 279*, 54663−54675.

BI051537Y